Organic LETTERS

Letter

pubs.acs.org/OrgLett

Applanatumin A, a New Dimeric Meroterpenoid from *Ganoderma applanatum* That Displays Potent Antifibrotic Activity

Qi Luo,[†,‡,⊥] Lei Di,[†,⊥] Wei-Feng Dai,[†,§] Qing Lu,[†] Yong-Ming Yan,[†,‡] Zhu-Liang Yang,[∥] Rong-Tao Li,[§] and Yong-Xian Cheng*[,†]

[†]State Key Laboratory of Phytochemistry and Plant Resources in West China, Kunming Institute of Botany and [∥]Laboratory for Plant Diversity and Biogeography of East Asia, Kunming Institute of Botany, Chinese Academy of Sciences, Kunming 650201, P. R. China

[‡]University of Chinese Academy of Sciences, Beijing 100049, P. R. China

[§]Faculty of Life Science and Technology, Kunming University of Science of Technology, Kunming 650500, P. R. China

Supporting Information

ABSTRACT: Applanatumin A (**1**), a novel meroterpenoid dimer, was isolated from the fungus *Ganoderma applanatum*. Its structure and absolute configuration were assigned on the basis of spectroscopic and computational data. Notably, **1** possesses a new hexacyclic skeleton containing a spiro[benzofuran-2,1′-cyclopentane] motif. A plausible pathway, involving a key Diels−Alder reaction, is proposed for the biosynthesis of **1**. Applanatumin A exhibits potent antifibrotic activity in TGF-β1-induced human renal proximal tubular cells.

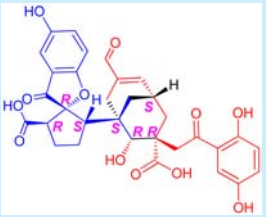

Organ fibrosis is a major medical issue because it can cause progressive dysfunction of multiple organs such as the heart, liver, lung, kidney, and skin and eventually death.[1−3] Unfortunately, no effective therapeutic approaches for fibrosis are currently available. Fibrosis can be initiated by a number of different factors, but regardless of its etiology, activation of the key profibrotic cytokine-transforming growth factor-β (TGF-β) is the common pathogenetic process. Excessive activation of TGF-β stimulates production and reduces degradation of extracellular matrix components, which are hallmarks of fibrosis. These events cause a gradual destruction of the function of normal tissue.[4,5] In addition, TGF-β signaling plays a central role in the epithelial−tomesenchymal transition in epithelial cells, which is also involved in organ fibrosis.[6,7] Therefore, targeting TGF-β and its associated products such as extracellular matrix proteins could be an effective strategy to retard the progress of organ fibrosis.

Ganoderma applanatum (Ganodermataceae) is a wood-decay fungus widely distributed in the world and typically found at the bases of tree stumps. Ecologically, this fungus is the common cause of decay and death of beech and poplar and, less often, other trees. In ancient China, several fungal species of the genus *Ganoderma* were recognized as the Lingzhi mushroom. Now many *Ganoderma* species are commonly sold in Chinese herbal medicine markets. *G. applanatum*, often considered to have a similar efficacy as *G. lucidum*, is used for the prevention and treatment of various chronic diseases in Chinese folk medicine. The remarkable curative effects of this fungus have been the subject of numerous chemical studies, which have demonstrated the presence of triterpenes, polysaccharides, lectins, sterols, alkaloids, polypeptides, amino acids, phenols, and coumarins.[8−10] Compounds isolated from *G. applanatum* are also found to have antioxidative, antiviral, antiobesity, antitumor, and immunomodulating activities.[11−13]

In one phase of our systematic studies of *Ganoderma* species, we have focused on *G. applanatum* and the discovery of compounds that are active against chronic kidney disease. The effort, described below, resulted in the characterization of a novel meroterpenoid dimer called applanatumin A (**1**), which we have shown possesses a novel spiro[benzofuran-2,1′-cyclopentane] ring system within its hexacyclic skeleton (Figure 1).

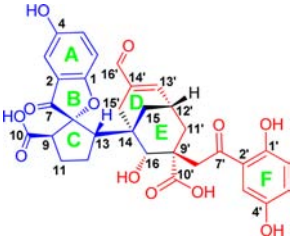

Figure 1. Structure of **1** (8*R*,9*R*,13*S*,14*S*,16*R*,9′*R*,12′*S*).

Furthermore, we have probed the antifibrotic activity of **1** in TGF-β1 induced human renal proximal tubular cells using Western blot analysis. Finally, a pathway for the biosynthesis of **1**, involving a key Diels−Alder reaction, is proposed.

Applanatumin A (**1**),[14] obtained from *G. applanatum* as an optically active yellow gum ($[\alpha]^{24}_{D}$ −95.4), possesses the molecular formula $C_{32}H_{30}O_{12}$ (18 degrees of unsaturation) derived from analysis of its HRESIMS, ^{13}C NMR, and DEPT spectra. The ^{1}H NMR spectrum (Table 1) of **1** contains two

Received: December 20, 2014
Published: February 23, 2015

DOI: 10.1021/ol503610b
Org. Lett. 2015, 17, 1110−1113

Table 1. ^{1}H (600 MHz) and ^{13}C NMR (150 MHz) Data of 1 in Methanol-d_4 (δ in ppm, J in Hz)

no.	δ_H	δ_C	no.	δ_H	δ_C
1		165.6 s	1′		156.3 s
2		123.0 s	2′		120.7 s
3	6.94 (d, 2.1)	108.7 d	3′	7.29 (d, 2.9)	115.5 d
4		154.4 s	4′		150.6 s
5	7.15 (dd, 8.9, 2.1)	128.1 d	5′	7.07 (dd, 8.9, 2.9)	125.8 d
6	7.14 (d, 8.9)	114.7 d	6′	6.81 (d, 8.9)	119.8 d
7		204.1 s	7′		205.1 s
8		99.7 s	8′a	3.78 (d, 17.7)	49.3 t
			8′b	3.00 (d, 17.7)	
9	3.21 (t-like, 8.6)	60.1 d	9′		55.0 s
10		174.9 s	10′		178.2 s
11a	2.09 (overlap)	27.7 t	11′a	2.39 (d, 13.8)	41.3 t
11b	1.95 (overlap)		11′b	1.73 (dd, 13.8, 7.4)	
12a	2.30 (m)	27.9 t	12′	1.92 (overlap)	42.0 d
12b	2.19 (m)				
13	2.61 (dd, 7.1, 5.2)	50.4 d	13′	6.54 (d, 5.0)	152.9 d
14		49.2 s	14′		140.7 s
15a	1.93 (overlap)	21.3 t	15′a	2.35 (d, 11.3)	18.8 t
15b	1.85 (dd, 13.5, 5.4)		15′b	2.09 (overlap)	
16	4.90 (overlap), 5.57[a] (s)	83.6 d	16′	9.33 (s)	196.0 s

[a]Recorded in pyridine-d_5 (800 MHz).

typical ABX proton coupling patterns {(δ_H 6.94, d, J = 2.1 Hz, H-3; δ_H 7.15, dd, J = 8.9, 2.1 Hz, H-5; δ_H 7.14, d, J = 8.9 Hz, H-6), (δ_H 7.29, d, J = 2.9 Hz, H-3′; δ_H 7.07, dd, J = 8.9, 2.9 Hz, H-5′; δ_H 6.81, d, J = 8.9 Hz, H-6′)}, and resonances for an aldehyde (δ_H 9.33, s, H-16′) and an olefinic proton (δ_H 6.54, d, J = 5.0 Hz, H-13′). Analysis of the ^{13}C NMR and DEPT spectra show that the 32 carbons in this substance are comprised of six methylenes, 12 methines (seven olefinics/aromatics, one aldehyde, one oxygenated), and 14 quaternary carbons (two ketones, two oxycarbonyls, seven olefinics/aromatics including four oxygenated, and three aliphatic including one oxygenated). The ^{1}H−^{1}H COSY spectrum (Figure 2) of **1** shows the presence of

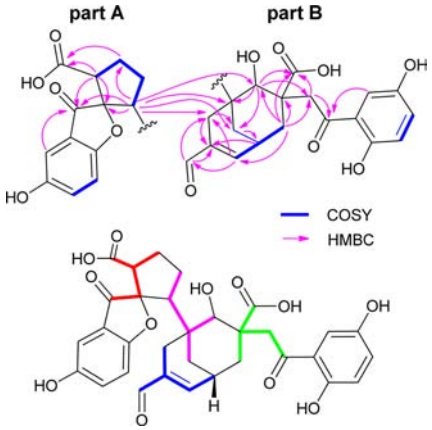

Figure 2. Key COSY and HMBC correlations of **1**; red, pink, blue, and green in **1** represent four independent isoprenyl moieties.

H-5/H-6, H-9/H-11/H-12/H-13, H-5′/H-6′, and H-11′/H-12′/H-13′ fragments. The structure of **1** was assigned mainly by using the results of an HMBC experiment, which show correlations between H-3, H-9 (δ_H 3.21), H-13 (δ_H 2.61)/C-7 (δ_C 204.1), and H-9, H-13/C-8 (δ_C 99.7). Consideration of their downfield shifts indicates that C-1 and C-8 are linked through an oxygen bridge. This suggests that two five-membered rings (B and C) are present as part of the spiro[benzofuran-2,1′-cyclopentane] motif ABC. Additional correlations between H-13/C-14 (δ_C 49.2), C-15 (δ_C 21.3) and C-16 (δ_C 83.6) indicate that the three carbon group C-14−C-15−C-16 is linked to C-13. Therefore, part A of **1** is extended to C-16 (Figure 2, pink line).

Part B of the natural product structure was assigned using additional HMBC observations. HMBC correlations from H-3′ and H-8′ (δ_H 3.78 and δ_H 3.00) to C-7′ (δ_C 205.1) and from H-8′ and H-6′ to C-2′ (δ_C 120.7) indicate that the aryl group in **1** (ring F) is linked to C-7′. Correlations from H-8′ to C-10′ (δ_C 178.2) and C-11′ (δ_C 41.3) and from H-11′ to C-8′ (δ_C 49.3), C-9′, and C-10′ suggest the presence of a prenyl group (Figure 2, green line). The existence of another prenyl moiety (Figure 2, blue line) is supported by the HMBC correlations from H-12′ (δ_H 1.92) to C-14′ (δ_C 140.7), from H-13′ (δ_H 6.54) to C-15′ (δ_C 18.8) and C-16′ (δ_C 196.0), and from H-15′ (δ_H 2.35 and δ_H 2.09) and H-16′ (δ_H 9.33) to C-14′. Further HMBC correlations between H-13/C-15′ and H-16/C-14 and C-15′ indicate that C-14 is linked to C-15′. Moreover, correlations between H-16/C-8′ and C-10′, H-11′/C-16 suggest the linkage of C-16 and C-9′. Unfortunately, ^{1}H−^{1}H COSY correlation between H-12′ and H-15 is uncertain due to the overlapping signals for Ha-15 and H-12′. Consideration of ^{1}H−^{1}H COSY correlations between H-11′/H-12′/H-13′ and HMBC correlations of H-15′, H-16/C-15 and H-15/C-12′ finally confirm the presence of two six-membered rings (rings D and E) in **1**. Thus, the planar structure of **1** was determined to be that shown in Figure 1.

The relative configurations at the stereogenic centers in **1** were assigned mainly by careful analysis of the ROESY spectrum (Figure 3). ROESY correlation between H-16/H-8′ suggests that these protons are positioned on the same side of ring E. The conformationally immobile bicyclo[3.3.1]non-2-ene ring system in **1** requires that CH-13′ and CH_2-15′ be oriented in the same direction on the E ring. Further correlation between H-16/Ha-15 (δ_H 1.93) and weak correlation between Hb-8′ (δ_H 3.00)/Ha-15 suggest that Ha-15 and H-16 are at the same side of ring E and also indicate the direction of bridgehead carbon (C-15), naturally allowing assignment of the relative configurations at C-12′ and

DOI: 10.1021/ol503610b
Org. Lett. 2015, 17, 1110−1113

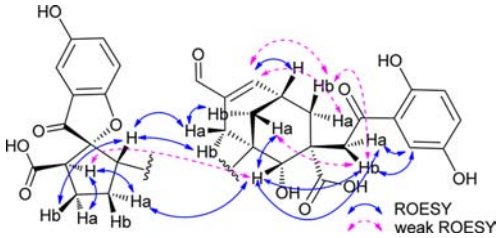

Figure 3. Key ROESY correlations of **1**.

C-14. Theoretically, free rotation about the C-13−C-14 single bond should be possible. However, the observed ROESY correlations between H-13/H-15′, H-16/Ha-12 (δ_H 2.30) indicate that this rotation is restricted as a consequence of steric hindrance. Under this circumstance, the observed ROESY correlations between H-16/H-9, Ha-12 and H-9/Ha-12 suggest that H-9 and H-13 are located on opposite sides of ring C. This conclusion is supported by the observations of ROESY interactions between H-13/Hb-11 (δ_H 1.95) and H-11a (δ_H 2.09)/H-9. Moreover, the correlation between H-13 and Hb-11 requires that the C ring adopt an envelope type conformation. The above findings enable assignments of the relative configurations at C-9, C-13, C-14, C-16, C-9′, and C-12′. The scarcity of effective correlations makes it impossible to assign the relative configuration at C-8 by using ROESY observations. Compound **1** was isolated as a gum which makes it impossible to obtain a single crystal for X-ray diffraction analysis. The limited amount of **1** also makes it challenging to obtain its derivative for further crystallographic analysis. As a result, computational methods were used to clarify the absolute configuration of **1** by comparing the experimental and time-dependent density-functional theory (TDDFT) calculated electronic circular dichroism (ECD) spectra. For this method, conformational analysis was initially performed by using Hyperchem conformational searching and the Amber molecular mechanics methods. The selected conformers were then optimized at the B3LYP/6-31+G(d,p) level in the gas phase by using the Gaussian09 software package.[15] Further ECD calculations were conducted at the B3LYP SCRF(PCM)/6-31+G(d,p)//B3LYP/6-31+G(d,p) level in MeOH solution. We found that the calculated weighted ECD spectrum of the conformers of **1** with 8*R*,9*R*,13*S*,14*S*,16*R*,9′*R*,12′*S* but not the other isomers (Supporting Information) is in good accordance with the experimental spectrum (Figure 4). Consequently, the absolute configuration of **1** was unambiguously assigned.

As indicated in Figure 1, the structure of applanatumin A appears to be composed of two parts including A represented by blue and B shown as red. With the exception of the 1,4-dihydroxybenzene group, the components of parts A and B in **1** appear to be terpene-like (Figure 2). On the basis of this analysis, it is possible to make the biogenetic proposal that both parts A and B are derived from the same precursor, geranylhydroquinone (Figure 4).[16] In the biosynthetic pathway, oxidation of geranylhydroquinone would yield a key intermediate A, which is further oxidized to give B and C. The monomer B can be cyclized via a conjugated addition to generate D. An interesting feature in the biosynthesis of **1** is the formation of spiro structure by a stereospecific phenol oxidative coupling.[17] Monomer G is formed by 1,3-hydrogen migration of F, and ring D is further formed by a Diels−Alder reaction between G and C. Finally, ring E in **1** is formed via reductive cyclization reaction.[18] Careful analysis of the novel skeleton of **1** suggests that three terminal methyls derived from geranylhydroquinone are oxidatively transformed in the biosynthetic route to three carbonyl groups, one of which is an aldehyde.

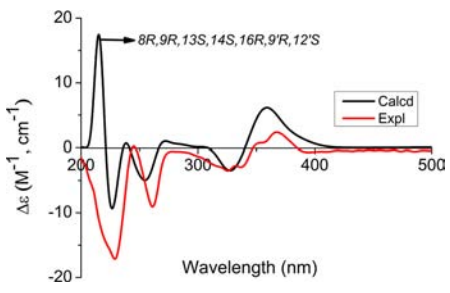

Figure 4. Calculated and experimental ECD spectra of **1** (red, at the B3LYP-SCRF(PCM)/6-31+G(d,p)//B3LYP/6-31+G(d,p) level in MeOH; black, experimentally observed in MeOH).

As mentioned above, a Diels−Alder reaction happened during the formation of **1**, a dubious question was that applanatumin A was formed as a natural or artificial product. LC−MS analysis of **1** in the crude extract (extracted by MeOH at room temperature, 3 × 12 h) found that **1** is a natural product supported by its diagnostic chromatographic and spectroscopic signals (Supporting Information).

Scheme 1. Plausible Pathway for the Biogenesis of 1

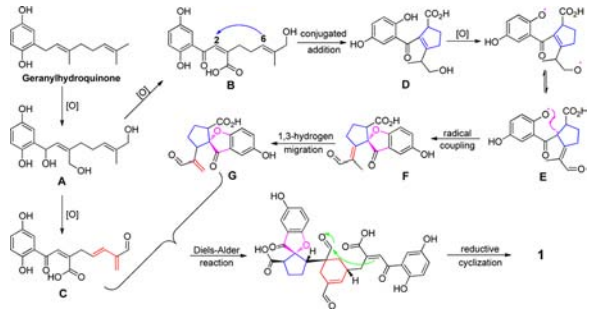

Among different types of fibrosis, kidney failure caused by renal fibrosis is of major concern. As a result, we have tested the antifibrotic ability of applanatumin A. Because excessive production of collagen I, fibronectin, and α-SMA is implicated in renal fibrosis, the antifibrotic action of **1** in TGF-β1-induced human renal proximal tubular cells was determined by using Western blot analysis targeting inhibition of these proteins. The results show that **1** causes a significant decrease in collagen I, fibronectin, and α-SMA expression in a dose-dependent manner (Figure 5). As mentioned above, TGF-β/Smads is considered to be the key profibrotic pathway, and overproduction of collagen I, fibronectin, and α-SMA might be associated with excessive activation of TGF-β/Smads. Consequently, inhibition of Smad2/3 phosphorylation by **1** was evaluated. The results show that phosphorylation of Smad2 and Smad3 is inhibited by **1** (Figure 6). To exclude the possibility that the effects of **1** are related to its cellular toxicity, the MTT exclusion test was carried out. The result shows that **1** is not toxic toward human renal proximal tubular cells at the concentrations ranging from 2.5 to 20 μM (data not shown). These findings suggest that applanatumin A represents a new structural scaffold in the search for antifibrotic drugs by targeting Smad3 phosphorylation (p-Smad3). To our knowledge, inhibitors of p-Smad3 are relatively rare, SIS3 as a blocker of p-Smad3 has been marketed as a tool drug.[19] Our discovery of six p-Smad3 inhibitors including

DOI: 10.1021/ol503610b
Org. Lett. 2015, 17, 1110−1113

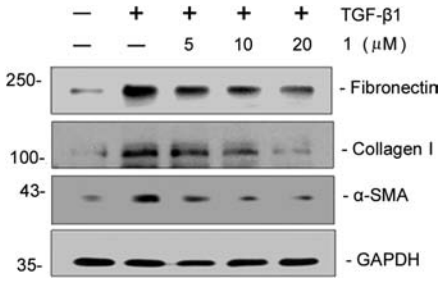

Figure 5. Compound **1** inhibits fibrogenic action of TGF-β1 in human renal proximal tubular cells. HKC-8 cells were incubated with TGF-β1 (5 ng/mL) for 48 h in the absence or presence of different concentrations (5−20 μM) of compound **1**. Cell lysates after various treatments as indicated were immunoblotted with antibodies against fibronecitn, collagen I, α-SMA, and GAPDH.

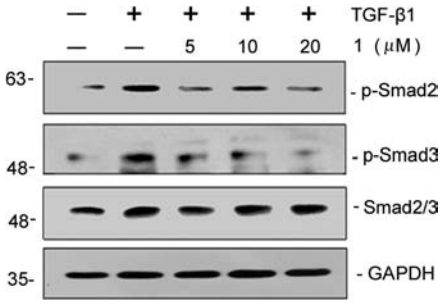

Figure 6. Compound **1** selectively blocks TGF-β1-mediated Smad2 and Smad3 phosphorylation in a dose-dependent manner. HKC-8 cells were treated with TGF-β1 (5 ng/mL) for 3 h in the absence or presence of different doses of **1** as indicated. Cell lysates after various treatments as indicated were immunoblotted with antibodies against phosphorylated Smad2, phosphorylated Smad3, total Smad2/3, and GAPDH.

GQ5,[20] lingzhiol,[21] (±)-aspongamide A,[22] cochlearols A and B,[23] and applanatumin A might contribute much to this field.

■ ASSOCIATED CONTENT

Supporting Information

1D, 2D NMR, and MS spectra, detailed isolation procedures, bioassay and computational methods. LC−MS analysis of **1** in the crude extract. This material is available free of charge via Internet at http://pubs.acs.org.

■ AUTHOR INFORMATION

Corresponding Author

*Phone/fax: +86-871-65223048. E-mail: yxcheng@mail.kib.ac.cn.

Author Contributions

$^{\perp}$Q.L. and L.D. contributed equally.

Notes

The authors declare no competing financial interest.

■ ACKNOWLEDGMENTS

This study was supported by the NSFC-Joint Foundation of Yunnan Province (U1202222), the National Natural Science Foundation of China (21472199), projects from the Center of Cooperative Innovation for South China Medicine of Yunnan Province, and Yong and Middle Aged Academic Leaders of Kunming.

■ REFERENCES

(1) Wynn, T. A. *J. Pathol.* **2008**, *214*, 199−210.
(2) Branton, M. H.; Kopp, J. B. *Microbes Infect.* **1999**, *1*, 1349−1365.
(3) Mauviel, A. *Methods Mol. Med.* **2005**, *117*, 69−80.
(4) Dirk, P.; Julia, B.; Ivonne, L.; Cornelia, K. M.; Carola, L.; Stefan, S. M.; Andreas, S.; Raimund, W. K.; Gunter, W. *Biochim. Biophys. Acta* **2009**, *1792*, 746−756.
(5) Blobe, G. C.; Schiemann, W. P.; Lodish, H. F. *New Engl. J. Med.* **2000**, *342*, 1350−1358.
(6) Kalluri, R.; Weinberg, R. A. *J. Clin. Invest.* **2009**, *119*, 1420−1428.
(7) Xu, J.; Lamouille, S.; Derynck, R. *Cell. Res.* **2009**, *19*, 156−172.
(8) Wang, F.; Liu, J. K. *Chem. Pharm. Bull.* **2008**, *56*, 1035−1037.
(9) Gan, K. H.; Kuo, S. H.; Lin, C. N. *J. Nat. Prod.* **1998**, *61*, 1421−1422.
(10) Li, Z. P.; Zhu, C. W.; Wu, P.; Wang, S. H.; Sun, Y. J. *Modern Food Sci. Technol.* **2013**, *8*, 1791−1795.
(11) Maja, K.; Anita, K.; Miomir, N.; Miroslav, M. V.; Nina, T.; Dragica, J.; Leo, V. G. *J. Food. Compost. Anal.* **2012**, *26*, 144−153.
(12) Kim, J. E.; Park, S. J.; Yu, M. H.; Lee, S. P. *J. Med. Food.* **2014**, *10*, 1086−1094.
(13) Jeong, Y. T.; Yang, B. K.; Jeong, S. C.; Kim, S. M.; Song, C. H. *Phytother. Res.* **2008**, *22*, 614−619.
(14) Applanatumin A (**1**): yellowish gum; $[\alpha]^{24}_{D}$ −95.4 (*c* 0.16, MeOH); UV (MeOH) λmax (logε) 370 (3.78), 224 (4.49) nm; CD (MeOH) $\Delta\varepsilon$228 −12.5, $\Delta\varepsilon$246 +0.05, $\Delta\varepsilon$261 −6.52, $\Delta\varepsilon$325 −2.60, $\Delta\varepsilon$366 +1.70; ESIMS *m*/*z* 605 $[M - H]^-$; HRESIMS *m*/*z* 605.1658 $[M - H]^-$ (calcd for $C_{32}H_{29}O_{12}$, 605.1695); ^{1}H and ^{13}C NMR data, see Table 1.
(15) Frisch, M. J.; Trucks, G. W.; Schlegel, H. B.; Scuseria, G. E.; Robb, M. A.; Cheeseman, J. R.; Scalmani, G.; Barone, V.; Mennucci, B.; Petersson, G. A.; Nakatsuji, H.; Caricato, M.; Li, X.; Hratchian, H. P.; Izmaylov, A. F.; Bloino, J.; Zheng, G.; Sonnenberg, J. L.; Hada, M.; Ehara, M.; Toyota, K.; Fukuda, R.; Hasegawa, J.; Ishida, M.; Nakajima, T.; Honda, Y.; Kitao, O.; Nakai, H.; Vreven, T.; Montgomery, J. A., Jr.; Peralta, J. E.; Ogliaro, F.; Bearpark, M.; Heyd, J. J.; Brothers, E.; Kudin, K. N.; Staroverov, V. N.; Keith, T.; Kobayashi, R.; Normand, J.; Raghavachari, K.; Rendell, A.; Burant, J. C.; Iyengar, S. S.; Tomasi, J.; Cossi, M.; Rega, N.; Millam, J. M.; Klene, M.; Knox, J. E.; Cross, J. B.; Bakken, V.; Adamo, C.; Jaramillo, J.; Gomperts, R.; Stratmann, R. E.; Yazyev, O.; Austin, A. J.; Cammi, R.; Pomelli, C.; Ochterski, J. W.; Martin, R. L.; Morokuma, K.; Zakrzewski, V. G.; Voth, G. A.; Salvador, P.; Dannenberg, J. J.; Dapprich, S.; Daniels, A. D.; Farkas, O.; Foresman, J. B.; Ortiz, J. V.; Cioslowski, J.; Fox, D. J. *Gaussian 09, Revision C.01*; Gaussian, Inc., Wallingford, CT, 2010.
(16) Aknin, M.; Dayan, T. L. A.; Rud, A.; Kashman, Y.; Gaydou, E. M. *J. Agric. Food Chem.* **1999**, *47*, 4175−4177.
(17) Chooi, Y. H.; Cacho, R.; Tang, Y. *Chem. Biol.* **2014**, *17*, 483−494.
(18) Zhang, G. T.; Zhang, W. J.; Zhang, Q. B.; Shi, T.; Ma, L.; Zhu, Y. G.; Li, S. M.; Zhang, H. B.; Zhao, Y. L.; Shi, R.; Zhang, C. S. *Angew. Chem., Int. Ed.* **2014**, *53*, 4840−4844.
(19) Jinnin, M.; Ihn, H.; Tamaki, K. *Mol. Pharmacol.* **2006**, *69*, 597−607.
(20) Ai, J.; Nie, J.; He, J. B.; Guo, Q.; Li, M.; Lei, Y.; Liu, Y. H.; Zhou, Z. M.; Zhu, F. X.; Liang, M.; Cheng, Y. X.; Hou, F. F. *J. Am. Soc. Nephrol.* **2014**, DOI: 10.1681/ASN.2014040363.
(21) Yan, Y. M.; Ai, J.; Zhou, L. L.; Chung, A. C. K.; Li, R.; Nie, J.; Fang, P.; Wang, X. L.; Luo, J.; Hu, Q.; Hou, F. F.; Cheng, Y. X. *Org. Lett.* **2013**, *15*, 5488−5491.
(22) Yan, Y. M.; Ai, J.; Shi, Y. N.; Zuo, Z. L.; Hou, B.; Luo, J.; Cheng, Y. X. *Org. Lett.* **2014**, *16*, 532−535.
(23) Dou, M.; Di, L.; Zhou, L. L.; Yan, Y. M.; Wang, X. L.; Zhou, F. J.; Yang, Z. L.; Li, R. T.; Hou, F. F.; Cheng, Y. X. *Org. Lett.* **2014**, *16*, 6064−6067.

DOI: 10.1021/ol503610b
Org. Lett. 2015, 17, 1110−1113